Automated segmentation of the skeleton in whole-body bone scans: Influence of difference in atlas

メタデータ	言語: eng
	出版者:
	公開日: 2017-10-03
	キーワード (Ja):
	キーワード (En):
	作成者:
	メールアドレス:
	所属:
URL	http://hdl.handle.net/2297/32474

Automated segmentation of the skeleton in whole-body bone scans : influence of difference in atlas

Akihiro Kikuchi[1], Masahisa Onoguchi[1]*, Hiroyuki Horikoshi[2], Karl Sjöstrand[3],

Lars Edenbrandt[4]

[1]School of Health Sciences, College of Medical, Pharmaceutical and Health   Sciences, Kanazawa University, Ishikawa

[2]Department of Diagnostic Radiology, Gunma Prefectural Cancer Center, Gunma, Japan

[3]Informatics and Mathematical modeling, Technical University of Denmark, Copenhagen, Denmark

[4]Department of Molecular and Clinical Medicine, Sahlgrenska Academy, Gothenburg University, Gothenburg, Sweden

*Correspondence to Masahisa Onoguchi, PhD, School of Health Sciences, College of Medical, Pharmaceutical and Health Sciences, Kanazawa University,5-11-80 Kodatuno, Kanazawa, Ishikawa 920-0942, Japan Tel: +81 762 652 500; fax: +81 762 344 351; e-mail: onoguchi@staff.kanazawa-u.ac.jp

3/22/2012; 5/16/2012; 5/30/2012

Abstract

Aim

Automated segmentation of the skeleton is the first step for quantitative analysis and computer-aided diagnosis (CAD) of whole-body bone scans. The purpose of this study was to examine the

influence of differences in skeletal atlas on the automated segmentation of skeletons in a Japanese patient group.

Method

The study was based on a bone scan CAD system that included a skeletal atlas obtained using 10 normal bone scans from European patients and 23 normal bone scans from Japanese patients. These were incorporated into the CAD system. The performance of the skeletal segmentation, based on either the European or the Japanese Atlas, was evaluated independently by three observers in a group of 50 randomly selected bone scans from Japanese patients.

Results

The skeletal segmentation was classified as correct in 41–44 of the 50 cases by the three observers using the Japanese atlas. The corresponding results were 15–18 of the 50 cases using the European atlas, and this difference was statistically significant ($P<0.001$). The anatomical areas most commonly classified as not correct were the skull, cervical vertebrae, and ribs.

Conclusion

Automated segmentation of the skeleton in a Japanese patient group was more successful when the CAD system based on a Japanese atlas was used than when the corresponding system based on a European atlas was used. The results of this study indicates that it is of value to use a skeletal atlas based on normal Japanese bone scans in a CAD system for Japanese patients.

Keywords:

bone scans, computer-aided diagnosis, skeletal segmentation

Introduction

Skeletal metastases are common in several tumors – for example prostate and breast cancer, and information about this is fundamentally important for the management and treatment of these patients. Furthermore, the presence and extent of metastases may greatly influence prognosis [1].

Whole-body bone scintigraphy is a sensitive modality that is frequently used to detect bone metastases. This modality has been in use for a long time at many nuclear medicine departments. It is a minimally invasive modality with a relatively short examination time. Interpretation of bone scans is based on visual reading by a physician, and the quality is therefore dependent on the physicians' experience in assessing the uptake and distribution of the radiopharmaceutical. Therefore, there may be differences in the diagnostic sensitivity and specificity between inexperienced and experienced nuclear medicine physicians. The quality of bone scan interpretations has been shown to vary considerably among physicians [2]. In a nation-wide survey including 37 observers, each of whom interpreted the same 59 bone scans, the sensitivities ranged from 52 to 100%. The study also showed moderate interobserver agreement between the observers.

To make interpretations of diagnostic images more objective, computer-aided diagnosis (CAD) systems have been developed for mammography, colonography, and myocardial perfusion scintigraphy and more recently for whole-body bone scans [3–8]. The CAD system for bone scans has also been developed to quantify the tumor burden in a bone scan index, which has been proven to be associated with survival in prostate cancer [1,9,10]. Automated segmentation of the skeleton is the first step in this CAD system, and a skeletal atlas obtained from normal bone scans is an important tool in this process. An assumption could be that it is of value to use a skeletal atlas based on normal Japanese bone scans in a system for Japanese patients as they might have smaller body size. It has been observed that if American and European standard values are used in myocardial scintigraphy, these normal values are

not always appropriate for a Japanese population in clinical practice [11]. Therefore, the purpose of this study was to examine the influence of differences in the skeletal atlas on the automated segmentation of skeletons in a Japanese patient group.

Materials and methods

Patients

The skeletal atlases were obtained using normal whole-body bone scans without metastases, high accumulation in the bladder, and technical problems during acquisition. The original skeletal atlas was based on 10 bone scans from patients examined at the Sahlgrenska University Hospital in Gothenburg, Sweden. The Japanese skeletal atlas was based on 23 bone scans from patients examined at the Gumma Prefectural Cancer Center, Japan.

The evaluation group consisted of 50 bone scans from 20 men (67 ± 3.6 years old) and 30 women (61 ± 2.4 years old), randomly selected from a group of 365 consecutive cases at the Gumma Prefectural Cancer Center in 2009. The group comprised 26 patients with breast cancer, 11 with prostate cancer, seven with lung cancer, two with gastric cancer, one with liver cancer, and three with other diagnoses.

Bone scintigraphy

Anterior and posterior whole-body bone scan images were acquired 3–5 h after an intravenous injection of 600 MBq (European cases) or 740 MBq (Japanese cases) technetium-99m methylene diphosphonate (GE Healthcare Ltd, Buckinghamshire, or FUJIFILM RI Pharma Co. Ltd., Japan). Dual-detector gamma-camera systems equipped with low-energy high-resolution parallel multichannel collimators were used [GE Maxxus; General Electric, Milwaukie, USA (European scans) or Siemens ECAM; Siemens, Erlangen, Germany (Japanese scans)]. The acquisition conditions of the whole-body

scan were set as follows: scan speed 10 cm/min (European scans) or 15 cm/min (Japanese scans), matrix

size 256×1024, energy window of energy peak 140 keV, and window width 15%.

Automated segmentation method

The bone scan CAD system used was the EXINI Bone system (EXINI Diagnostics AB, Lund,

Sweden), which has been presented elsewhere [8]. A Japanese version, BONENAVI, of this system has

Fig. 1
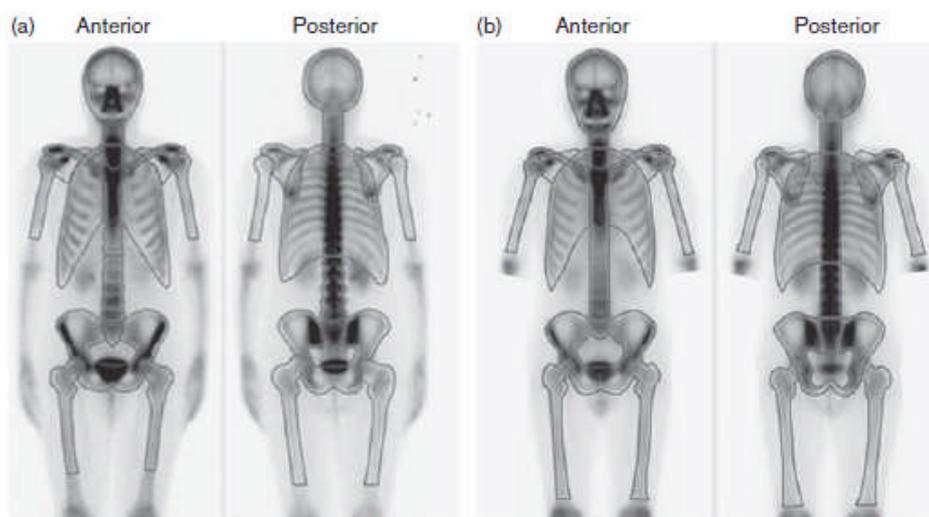
Skeletal atlases based on normal bone scans from (a) 10 European patients and (b) 23 Japanese patients.

been developed. The skeleton is delineated automatically by fitting a manually delineated atlas,

consisting of one anterior and one posterior image to the skeleton (Fig. 1).

The atlas was constructed by fitting each of the normal scans to a fictitious normal subject with

the average anatomy and intensity of the normal group. The atlas is manually segmented into 12

separate anatomical regions: skull, cervical vertebrae, thoracic vertebrae, lumbar vertebrae, sacrum,

pelvis, ribs, scapula, humerus, and femur in both the anterior and posterior images; and clavicle and

sternum in the anterior image. The transformation between the atlas and a patient skeleton is established

using a technique for nonrigid image registration [12]. This transformation can be used to segment the patient skeleton. Once the transformation from the atlas to the patient skeleton is acquired, the manual delineation of the atlas image can be transformed accordingly. If the transformed atlas fully corresponds to the patient skeleton, an accurate segmentation of the patient skeleton is provided. The registration algorithm is a slightly modified version of the Morphon method [13]. This method proceeds in iterations, wherein each iteration brings the atlas image into closer correspondence with the patient image.

The Morphon is a proper image registration method yielding correspondences at every pixel. Other image segmentation methods such as active shape models find an anatomically plausible shape along the object boundaries. For bone scan images, such methods may have trouble in certain regions of the skeleton where clear boundary image information is lacking, such as the ribs. The Morphon takes the entire image into account and not just the boundaries of the segmentation.

The Morphon registration algorithm was devised by Knutsson and Andersson [13]. Petterson *et al.* [14] present an application of the Morphon to the segmentation of the pelvis from computed tomographic images. The Morphon method yields the original data that are approximated to the target data by iterative deformation. Actual analysis consists of four steps: deformation of the source image according to the current accumulated deformation field, estimation of a new deformation field, deformation field regularization, and the addition of the regularized deformation field to the accumulated field [12].

Image deformation

This deformation is performed using a standard image warping technology.

Deformation field estimation

It is estimated from local measurement of the phase difference between the source and destination images that a new deformation field is formed. Image phase has been estimated using a complex filter is sensitive to edge ridge of intensity, valley, in a specific direction.

Deformation field regularization

Evaluation of the deformation field, without giving a sense of model spatial dependence in the deformation vector, does not necessarily reinforce the smoothness. Instead, it has been incorporated into the subsequent step of regularization that is focused upon in this study. The Morphon method, as a result of elastic deformation, suggests that the filtering approach is known as the normalized average (13.11).

The matrix for each component of the deformation field was convolved with a Gaussian kernel.

Deformation field accumulation

The resultant deformation field regularization will be added to the total deformation field that describes the conversion of the original image from the source to the target.

Two versions of the CAD system were developed, one using the European atlas and the other using the Japanese atlas. The bone scans of the evaluation group were analyzed using both versions.

Evaluation method

Three observers familiar with bone scan interpretation, who were blinded to the information of the atlas used (European or Japanese), independently classified the quality of the automated segmentation for all bone scans of the evaluation group as correct (the observer would manually have segmented the skeleton in exactly the same way) or not correct (some discrepancies between automated and manual segmentation would have occurred). For each case a classification was made for the complete bone scan and for the following 14 anatomical regions: skull, cervical vertebrae, thoracic vertebrae, lumbar

vertebrae, sacrum, right upper limb, left upper limb, left rib, right rib, sternum, left pelvic region, right pelvic region, left lower limb, and right lower limb.

Statistical methods

The discrepancy rate was calculated for each evaluation image obtained using the European and Japanese atlases, and the differences in discrepancy rates were tested by the Obuchowski method.

Results

The three observers on average classified the automated segmentation based on the Japanese atlas as correct in 86% of the 50 cases (Tables 1 and 2). The corresponding result using the European atlas was 33%, and this difference was statistically significant ($P<0.001$). Three cases presented in Fig. 2 illustrate these results.

Table 1 Automated segmentation based on the European and Japanese atlas

Observer	Atlas	Number of patients		Discrepancy rate (%)[a]	P value[†]
		Correct	Not correct		
A	European	17	33	66.0 (52.2, 77.6)	<0.001
	Japan	41	9	18.0 (9.8, 30.8)	
B	European	18	32	64.0 (50.1, 75.9)	<0.001
	Japan	44	6	12.0 (5.6, 23.8)	
C	European	15	35	70.0 (56.2, 80.9)	<0.001
	Japan	44	6	12.0 (5.6, 23.8)	

Patient results.
[a]Data in parentheses are 95% confidence intervals by the Wilson's score method.
[†]P values were calculated by the McNemar test.

The agreement among the classifications made by the three observers was very good. A pairwise comparison among the three observers resulted in κ values of 0.94, 0.84, and 0.89 for the European atlas and 0.74, 0.74, and 1.00 for the Japanese atlas. The anatomical areas most commonly classified as not correct were the skull, cervical vertebrae, and ribs (Table 3). In addition, as an Appendix 1, we show the results of the three observers for all cases (Appendix).

Table 2 Proportion of not correct segmentation for each anatomical region based on the European and Japanese atlas in 50 cases and three readers

Region	Reader	Proportion of not correct (%)[a]	
		European	Japanese
Skull	A	40.0 (27.6, 53.8)	16.0 (8.3, 28.5)
	B	34.0 (22.4, 47.8)	10.0 (4.3, 21.4)
	C	36.0 (24.1, 49.9)	10.0 (4.3, 21.4)
Cervical vertebra	A	40.0 (27.6, 53.8)	14.0 (7.0, 26.2)
	B	34.0 (22.4, 47.8)	10.0 (4.3, 21.4)
	C	36.0 (24.1, 49.9)	10.0 (4.3, 21.4)
Thoracic vertebrae	A	8.0 (3.2, 18.8)	0.0 (0.0, 7.1)
	B	8.0 (3.2, 18.8)	0.0 (0.0, 7.1)
	C	8.0 (3.2, 18.8)	0.0 (0.0, 7.1)
Lumbal vertebrae	A	8.0 (3.2, 18.8)	0.0 (0.0, 7.1)
	B	8.0 (3.2, 18.8)	0.0 (0.0, 7.1)
	C	8.0 (3.2, 18.8)	0.0 (0.0, 7.1)
Left upper limb	A	8.0 (3.2, 18.8)	2.0 (0.4, 10.5)
	B	8.0 (3.2, 18.8)	2.0 (0.4, 10.5)
	C	10.0 (4.3, 21.4)	2.0 (0.4, 10.5)
Right upper limb	A	8.0 (3.2, 18.8)	4.0 (1.1, 13.5)
	B	8.0 (3.2, 18.8)	2.0 (0.4, 10.5)
	C	8.0 (3.2, 18.8)	2.0 (0.4, 10.5)
Left ribs	A	44.0 (31.2, 57.7)	2.0 (0.4, 10.5)
	B	46.0 (33.0, 59.6)	0.0 (0.0, 7.1)
	C	60.0 (46.2, 72.4)	0.0 (0.0, 7.1)
Right ribs	A	42.0 (29.4, 55.8)	2.0 (0.4, 10.5)
	B	44.0 (31.2, 57.7)	0.0 (0.0, 7.1)
	C	50.0 (36.6, 63.4)	0.0 (0.0, 7.1)
Sternum	A	8.0 (3.2, 18.8)	0.0 (0.0, 7.1)
	B	8.0 (3.2, 18.8)	0.0 (0.0, 7.1)
	C	8.0 (3.2, 18.8)	0.0 (0.0, 7.1)
Sacrum	A	8.0 (3.2, 18.8)	0.0 (0.0, 7.1)
	B	8.0 (3.2, 18.8)	0.0 (0.0, 7.1)
	C	8.0 (3.2, 18.8)	0.0 (0.0, 7.1)
Left pelvis	A	8.0 (3.2, 18.8)	0.0 (0.0, 7.1)
	B	8.0 (3.2, 18.8)	0.0 (0.0, 7.1)
	C	10.0 (4.3, 21.4)	0.0 (0.0, 7.1)
Right pelvis	A	8.0 (3.2, 18.8)	0.0 (0.0, 7.1)
	B	8.0 (3.2, 18.8)	0.0 (0.0, 7.1)
	C	10.0 (4.3, 21.4)	0.0 (0.0, 7.1)
Left lower limb	A	8.0 (3.2, 18.8)	0.0 (0.0, 7.1)
	B	8.0 (3.2, 18.8)	0.0 (0.0, 7.1)
	C	8.0 (3.2, 18.8)	0.0 (0.0, 7.1)
Right lower limb	A	8.0 (3.2, 18.8)	0.0 (0.0, 7.1)
	B	8.0 (3.2, 18.8)	0.0 (0.0, 7.1)
	C	10.0 (4.3, 21.4)	0.0 (0.0, 7.1)

[a]Numbers in parentheses are 95% confidence intervals.

Table 3   Discrepancy rate of each anatomical region based on the European and Japanese atlas in 50 cases and three observers

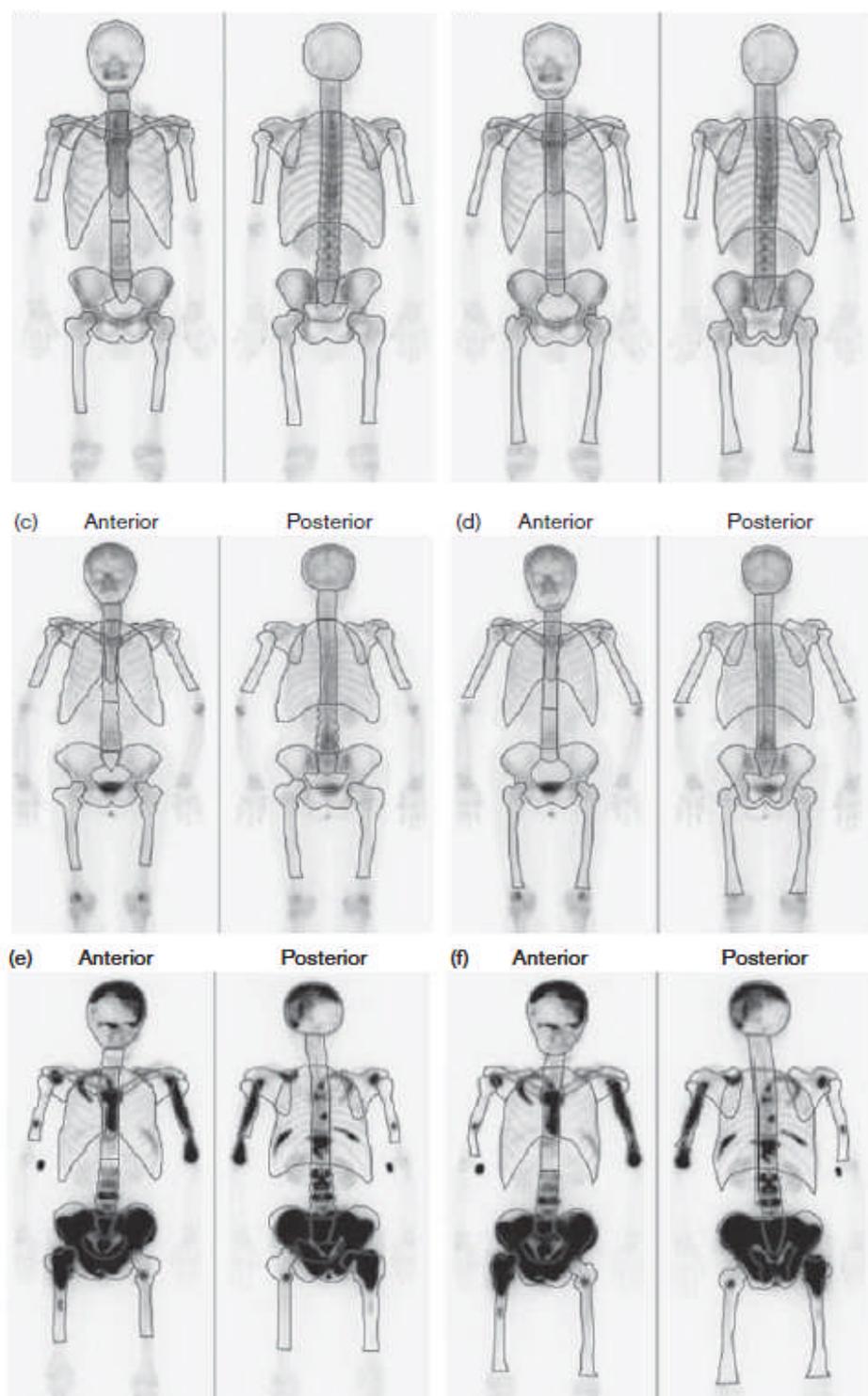| Region	Discrepancy rate (%)					
	European atlas			Japanese atlas		
	Observer A	Observer B	Observer C	Observer A	Observer B	Observer C
Skull	40.0	34.0	36.0	16.0	10.0	10.0
Cervical vertebra	40.0	34.0	36.0	14.0	10.0	10.0
Thoracic vertebrae	8.0	8.0	8.0	0.0	0.0	0.0
Lumbar vertebrae	8.0	8.0	8.0	0.0	0.0	0.0
Left upper limb	8.0	8.0	10.0	2.0	2.0	2.0
Right upper limb	8.0	8.0	8.0	4.0	2.0	2.0
Left ribs	44.0	46.0	60.0	2.0	0.0	0.0
Right ribs	42.0	44.0	50.0	2.0	0.0	0.0
Sternum	8.0	8.0	8.0	0.0	0.0	0.0
Sacrum	8.0	8.0	8.0	0.0	0.0	0.0
Left pelvis	8.0	8.0	10.0	0.0	0.0	0.0
Right pelvis	8.0	8.0	10.0	0.0	0.0	0.0
Left lower limb	8.0	8.0	8.0	0.0	0.0	0.0
Right lower limb	8.0	8.0	10.0	0.0	0.0	0.0

Discussion

Automated segmentation of the skeleton in a Japanese patient group was more successful when a CAD system based on a Japanese atlas was used than when the corresponding system based on a European atlas was used. The physical differences between races may at least partly cause these differences. The difference in count intensity due to the difference in body thickness may have affected body contouring, especially in the thorax or cervical-vertebra area where the difference in thickness was large.

Differences due to race in the mass of the skeleton have been reported, but the data must be interpreted with care because of the small number of cases studied and the differences in the selection of patients, such as differences in age [16]. There are, however, data that indicate that skeletal masses are greater in blacks than in whites of the same sex. Therefore, there may be differences in skeletal masses between Japanese and European patients as well, and the approach to use different atlases seems reasonable.

Differences in the physical constitution, especially in the thickness of the trunk between Japanese and European patients, may result in different count intensities. Differences in count intensities and not only in the shape of the skeleton may influence the computer-based segmentation process. The Japanese and European atlases differ, especially for the skull and ribs. Figure 3 shows a bone scan from a patient with breast cancer and multiple bone metastases. The hotspot in the mandible is falsely labeled as a cervical lesion on the basis of the European atlas but is correctly labeled as a skull lesion on the basis of the Japanese atlas. An incorrect localization of hotspots may cause both false diagnosis and inaccurate quantification of the bone scan index.

Fig. 2

(c)   Anterior   Posterior   (d)   Anterior   Posterior

(e)   Anterior   Posterior   (f)   Anterior   Posterior

Examples of automated segmentation based on the European atlas and Japanese atlas. The segmentation of case 1 was classified as 'correct' for both the (a) European and (b) Japanese atlases. The second case was classified as 'not correct' for the (c) European atlas. The segmentation of the skull and the lower ribs was not accurate. The corresponding segmentation for the (d) Japanese atlas was classified as 'correct'. The third case was classified as 'not correct' for both the (e) European and (f) Japanese atlases because of segmentation problems in the skull, upper limbs, pelvis, and femur.

Fig. 3
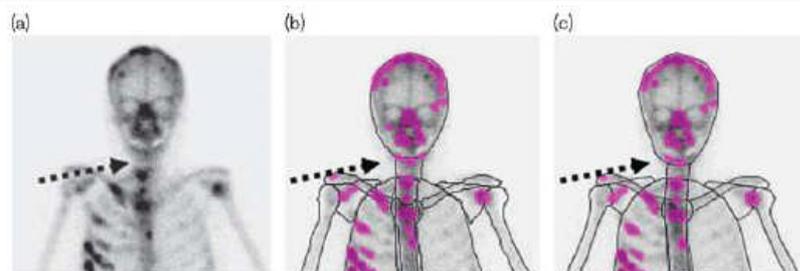
Bone scan from a patient with breast cancer and multiple metastases, presented as (a) raw image, and with hotspots marked together with (b) European and (c) Japanese atlases. The mandibular hotspot is falsely classified as a cervical lesion using the European atlas but is correctly classified using the Japanese atlas.

Conclusion

The results of this study indicate that it is of value to use a skeletal atlas based on normal Japanese bone scans in a CAD system for Japanese patients.

Acknowledgements

Conflicts of interest

A.Kikuchi is employed in FUJIFILM RI Pharma Co. Ltd., which distributes the software BONENAVI, and Sjöstrand and Edenbrandt are employed in EXINI Diagnostics AB, Lund, Sweden, which has developed the EXINI bone and BONENAVI software.

Appendix 1 Uncorrected region on the basis of automated segmentation in each subject

ID	European			Japanese		
	Observer A	Observer B	Observer C	Observer A	Observer B	Observer C
1	1–14	1–14	1–14	1, 2	1, 2	1, 2
2	ND	ND	ND	ND	ND	ND
3	1–14	1–14	1–14	ND	ND	ND
4	ND	ND	1, 2, 7, 8	ND	ND	ND
5	ND	ND	ND	ND	ND	ND
6	1, 2, 7, 8	7, 8	7, 8	ND	ND	ND
7	1–14	1–14	1–14	7, 8	ND	ND
8	1, 2	7, 8	7, 8	ND	ND	ND
9	ND	ND	ND	ND	ND	ND
10	1–14	1–14	1–14	1, 2	ND	ND
11	7	7	7	ND	ND	ND
12	7, 8	7, 8	7	ND	ND	ND
13	1, 2	1, 2	1, 2	1, 5	5	5
14	7, 8	7, 8	7, 8	ND	ND	ND
15	7, 8	7, 8	7, 8	ND	ND	ND
16	1, 2	1, 2	1, 2, 7, 8	1, 2, 6	1, 2	1, 2
17	ND	ND	ND	ND	ND	ND
18	ND	ND	ND	ND	ND	ND
19	1, 2	1, 2	1, 2	1, 2	1, 2	1, 2
20	7, 8	7, 8	7, 8	ND	ND	ND
21	7, 8	7, 8	7, 8, 11, 12	ND	ND	ND
22	ND	ND	ND	ND	ND	ND
23	ND	ND	ND	ND	ND	ND
24	ND	ND	ND	ND	ND	ND
25	1, 2	1, 2	1, 2, 7, 8	ND	ND	ND
26	1, 2, 7, 8	7, 8	7, 8	ND	ND	ND
27	1, 2	1, 2	1, 2	1, 2	1, 2	1, 2
28	1, 2	1, 2	1, 2	ND	ND	ND
29	1, 2, 7, 8	1, 2, 7, 8	1, 2, 7, 8	ND	ND	ND
30	7, 8	ND	ND	ND	ND	ND
31	1, 2	1, 2	1, 2, 5, 14	1, 2, 6	1, 2, 6	1, 2, 6
32	7, 8	7, 8	7, 8	ND	ND	ND
33	ND	ND	7	ND	ND	ND
34	ND	ND	ND	ND	ND	ND
35	ND	ND	7	ND	ND	ND
36	7, 8	7, 8	1, 2, 7, 8	ND	ND	ND
37	ND	ND	ND	ND	ND	ND
38	ND	ND	ND	ND	ND	ND
39	7, 8	7, 8	7, 8	ND	ND	ND
40	1, 2, 7, 8	1, 2, 7, 8	1, 2, 7, 8	ND	ND	ND
41	7, 8	7, 8	7, 8	ND	ND	ND
42	1, 2,	1, 2	1, 2, 7	ND	ND	ND
43	1, 2, 7, 8	1, 2, 7, 8	7, 8	1, 2	ND	ND
44	ND	ND	ND	ND	ND	ND
45	1, 2	1, 2	1, 2, 7, 8	ND	ND	ND
46	7, 8	7, 8	7, 8	ND	ND	ND
47	ND	ND	ND	ND	ND	ND
48	7, 8	7, 8	7, 8	ND	ND	ND
49	ND	ND	ND	ND	ND	ND
50	1, 2	1, 2, 7, 8	1, 2, 7, 8	ND	ND	ND

ND, not detected the region of uncorrected segmentation.
Anatomical regions; 1, cranial bone; 2, cervical vertebra; 3, vertebrae thoracic; 4, lumbar; 5, right upper limb; 6, left upper limb; 7, left rib; 8, right rib; 9, sternum; 10, sacral bone; 11, left pelvic region; 12, right pelvic region; 13, left lower limb; 14, right lower limb.

References

1. Sabbatini P, Larson SM, Kremer A, Zhang ZF, Sun F, Yeung H, *et al.*: Prognostic significance of extent of disease in bone in patients with androgen-independent prostate cancer. J Clin Oncol 1999;17:948-957

2. Sadik M, Suurkula M, Hoglund P, Jarund A, Edenbrandt L Quality of planar whole-body bone scan interpretations: a nationwide survey. Eur J Nucl Med Mol Imaging. 2008;35:1464–1472

3. Doi K .Computer-aided diagnosis in medical imaging: historical review, current status and future potential. Comput Med Imaging Graph. 2007;31:198–211

4. Cupples TE, Cunningham JE, Reynolds JC .Impact of computer-aided detection in a regional screening mammography program. Am J Roentgenol. 2005;185:944–950

5. Freer TW, Ulissey MJ .Screening mammography with computer-aided etection: prospective study of 12,860 patients in a community breast center. Radiology. 2001;220:781–786

6. Summers RM, Handwerker LR, Pickhardt PJ, Van Uitert RL, Deshpande KK, Yeshwant S, *et al.* Performance of a previously validated CT colonography computer-aided detection system in a new patient population. Am J Roentgenol. 2008;191:168-174

7. Tägil K, Bondouy M, Chaborel JP, *et al.* A decision support system improves the interpretation of myocardial perfusion imaging. Eur J Nucl Med Mol Imaging. 2008;35:1602–1607

8. Sadik M, Hamadeh I, Nordblom P, Suurkula M,HöglundP,Ohlsson M,et al.Computer-assisted diagnosis of planar whole-body bone scans J Nucl Med2008;49:1958–1965

9. Imbriaco M, Larson SM, Yeung HW, Mawlawi OR, Erdi Yusuf, Venkatraman ES**,***et al.*: A new parameter for measuring metastatic bone involvement by prostate cancer: the bone scan index. Clin Cancer Res. 1998;4:1765-1772

10. Ulmert D, Kaboteh R, Fox JJ, Savage C, Evans MJ, Lilja H, *et al.* A novel automated platform to quantify the extent of skeletal tumor involvement in prostate cancer patients with bone scan index. Eur Urol2012; 62:78-84

11. Nakajima K, Okuda K, Kawano M, Matsuo S, Slomka P, Germano G, Kinuya S .The importance of population-specific normal database for quantification of myocardial ischemia: comparison between Japanese 360 and 180-degree databases and a US database. J Nucl Cardiol. 2009;16:422-430

12. Sjöstrand K, Ohlsson M, Edenbrandt L .Statistical regularization of deformation fields for atlas-based segmentation of bone scintigraphy images. MICCAI 2009, Lecture Notes in Computer Science,2009, 5761/2009, 664-671 DOI: 10.1007/978-3-642-04268-3_82.

13. Knutsson H, Andersson M .Morphons: Paint on priors and elastic canvas for segmentation and registration. In: Scandinavian Conference on Image Analysis, SCIA; Joensuu, Finland; 19–22 June 2005.

14. Pettersson, J, Knutsson, H, Borga, M. Automatic hip bone segmentation using non-rigid registration. In: Proceedings of the IEEE 18th International Conference on Pattern Recognition, Hong Kong, China, 2006, pp.946–949.

15. Valentin J,Basic anatomical and physiological data for use in radiological protection: reference values. ICRP Publication 89. Ottawa, Canada: The International Commission on Radiological Protection; p.171.